Sepehr, Amir; Pouresmaeil, Mobina; Pouresmaeil, Edris

Enhancing Transient Stability of Power Synchronization Control via Deep Learning

Published in:
Proceedings of the 23rd European Conference on Power Electronics and Applications, EPE'21 ECCE Europe

DOI:
10.23919/EPE21ECCEEurope50061.2021.9570417

Published: 25/10/2021

Document Version
Peer-reviewed accepted author manuscript, also known as Final accepted manuscript or Post-print

Please cite the original version:
Sepehr, A., Pouresmaeil, M., & Pouresmaeil, E. (2021). Enhancing Transient Stability of Power Synchronization Control via Deep Learning. In Proceedings of the 23rd European Conference on Power Electronics and Applications, EPE'21 ECCE Europe IEEE. https://doi.org/10.23919/EPE21ECCEEurope50061.2021.9570417

Enhancing Transient Stability of Power Synchronization Control via Deep Learning

Amir Sepehr, Mobina Pouresmaeil, Edris Pouresmaeil
Department of Electrical Engineering and Automation, Aalto University
Espoo, Finland
amir.sepehr@aalto.fi, mobina.pouresmaeil@aalto.fi, edris.pouresmaeil@aalto.fi

Keywords

«Converter control», «Grid-forming converter», «Low-inertia grid», «Machine learning», «Synchronization stability».

Abstract

Transient stability of grid-connected converters has become a critical threat to the power systems with high integration level of renewable power generations. Thus, this paper aims to study the transient stability of power synchronization control (PSC) and propose a developed control system by employing deep learning methods. In order to extract and predict the voltage trajectory of the grid-connected converter system, a long short-term memory (LSTM) network has been trained and then integrated to PSC for adapting the synchronization loop of the converter to the grid condition. In the proposed control system, active power reference and internal voltage of the converter are updated dynamically to both satisfy the low voltage ride through (LVRT) requirements of the grid and prevent the loss of synchronization of the converter. The developed control system is validated by time-domain simulations.

Introduction

Alongside the advances in renewable energy technologies, grid-connected converters have played an indispensable role in the rapid integration of renewable energy sources (RES) into the power system [1]. Starting with the pathbreaking vector current control for grid-connected converters, new concerns have appeared about the integration of RES into weak power grids [2]. The main concern is that the standard vector current control fails to ensure converter stability when the converter is connected to a weak high-impedance grid [3]. Basically, voltage and frequency volatility are the main characteristics of weak power grids which jeopardize stability of the converter and power quality of the grid [4], [5].

Over time, control schemes based on emulation of synchronous generators have been introduced to provide supportive services for weak grids as well as maintaining the converter stability under weak grid operating condition [6], [7]. Accordingly, the emulation of synchronous machine dynamics has ramped up to fully functional control schemes including virtual synchronous machine (VSM) also known as synchronverter, synchronous power controller (SPC), and power synchronization control (PSC) [8]. PSC offers seamless integration of RES into weak grids and allows delivering active power between remote points by the grid-connected converters [9]. Thus, this paper focuses on PSC which is tailored for weak and very weak power grids and has been developed constantly in recent years.

Stability of grid-connected converters can be categorized into two main aspects, small-signal stability and transient stability. Small-signal stability of PSC has been studied through Jacobian transfer matrix and impedance models in [2], [9]. Similarly, transient stability of PSC has been studied based on design-oriented transient stability analysis and time-domain simulation in [10]. The conducted researches provided insight into the stability margins of PSC in the situation of severe disturbances and grid faults. In addition, in [8] a modified PSC scheme has been proposed which introduces a power-angle anti-windup function in order to adjust the active power reference of the converter during grid faults and enhance the transient stability of the converter. The modified PSC uses a back-calculation method for adjusting the active-power error which is the input of the synchronization loop of the converter. As a result, the power-angle of the converter would be limited for preventing the loss of synchronization.

However, the modified PSC structure has a poor performance in case of phase shift occurrence in the grid voltage. Furthermore, the low voltage ride through (LVRT) requirements would not be satisfied by the modified controller proposed in [8].

Therefore, considering the high variety of operating conditions and grid faults, and the voltage volatility of weak grids, it is becoming essential to develop machine learning-based solutions for adapting the converter control system to the operating condition of the grid. Thus, this paper aims to employ machine learning tools alongside transient stability analysis of grid-connected converters to improve the transient stability of PSC during grid faults.

In this paper, long short-term memory (LSTM) architecture, a powerful family of recurrent neural networks that is designed to predict sequences and time-series, is adopted to predict the behavior of the grid voltage and adapt the active power reference and internal voltage reference of the converter for both satisfying the LVRT requirements of the grid and improving transient stability of the converter. The LSTM layer learns long-term dependencies among time steps in time series and sequence data [11], [12]. Resulting from long-term information preservation and short-term input skipping, LSTM is capable of analyzing and predicting the behavior of the grid voltage during faults. Consequently, the main contribution of this paper is to develop the PSC scheme for enhancing the transient stability of converter based on conducting theoretical analysis and employing deep learning tools.

The rest of this paper is organized as follows. First, the transient stability of PSC during grid faults is discussed, then the voltage behavior of the connection point of the converter during grid faults is studied and a deep learning method for extracting and predicting the voltage trajectory is proposed. Eventually, the LSTM-integrated PSC scheme is introduced, and time-domain simulations are presented to confirm the effectiveness of the developed control system.

Transient stability of PSC during grid faults

PSC for grid-connected converter was first introduced in [2] and the description of the control scheme has been presented in [9] and robust design of the controller has been presented in [13]. The control system of a three-phase grid-connected converter with PSC is depicted in Fig. 1. Synchronization with the grid voltage and control of delivering active power to the grid are achieved by the power synchronization loop expressed by:

$$\delta = K_{ip} \int (P_{ref} - P) \tag{1}$$

$$\theta = K_{ip} \int (P_{ref} - P) + \omega_0 t \tag{2}$$

where δ is the power angle of the converter, K_{ip} is the integral gain of the power synchronization loop, and θ is the angle of the converter's internal voltage. The converter is connected to the grid via an inductive filter. The reference of the active power is denoted by P_{ref}, the delivered active power to the grid is expressed by P, and ω_0 is the grid frequency. The power angle δ represents the phase difference between the converter voltage and the grid voltage. Amplitude of the voltage at the terminal of the converter and the delivered reactive power are controlled by regulating the internal voltage of converter via ΔV by:

$$\mathbf{v}_{ref}^{dq} = (V_0 + \Delta V) - D(s)\mathbf{i}^{dq} \tag{3}$$

$$D(s) = \frac{R_d s}{s + \omega_b} \tag{4}$$

where, V_0 is the rated voltage of the system, $\mathbf{v}_{ref}^{dq}$ and $\mathbf{i}^{dq}$ are reference voltage vector and current vector of converter in synchronous reference frame (SRF), respectively; and $D(s)$ is a high-pass filter for active damping of high-order harmonic components of the converter current. The bandwidth and the gain of the active-damping block are represented by ω_b and R_d, respectively. It should be noted that for smooth initial synchronization with the grid voltage, a backup PLL is embedded in the control system as well. Linearized small-signal model that expresses the relationship between the delivered active power and the power-angle of the converter can be expressed by $\Psi_{P\delta}(s)$ derived in [2], [9] and reported below:

$$\Psi_{P\delta(s)} = \frac{\Delta P}{\Delta \delta} = \frac{\gamma_2 s^2 + \gamma_1 s + \gamma_0}{((x_{eq} / \omega_0)s + r_{eq})^2 + (x_{eq})^2} \tag{5}$$

where the coefficients of the numerator γ_0, γ_1, and γ_2 are dependent on the operating point of the converter as discussed in [2], x_{eq} and r_{eq} are the equivalent reactance and equivalent resistance of the system, respectively. The transmission zeros of $\Psi_{P\delta}(s)$ restrain the bandwidth of the control system. In fact, the bandwidth of the control system is dependent on the operating point of the converter as reported in [9], [12]. Zeros of the transfer function reach the origin when the power-angle of the converter equals to $\pm\pi/2$. Accordingly, to provide sufficient gain and bandwidth for the synchronization loop, operating close to $\delta=\pm\pi/2$ is strongly inappropriate.

Dynamic Representation of synchronization loop during grid faults

A three-phase grid-connected converter system is shown in Fig. 1 (a), where the converter is connected to the infinite bus via a transformer and two parallel lines modelled by x_{tr}, and $x_1 \| x_2$, respectively. It is assumed that the dc-bus of the converter is regulated at a constant voltage by an energy storage system. Since the shunt capacitances show insignificant influence on the transient stability of the system, the output filter of converter is modelled by a reactance x_f. The converter is connected to a high-impedance weak grid, in this case the control system should regulate the voltage of the point of common coupling (PCC) and regulate the delivered active power.

Dynamic representation of the power synchronization loop can be expressed by a first-order nonlinear equation as:

$$\dot{\delta} = K_{ip}(P_{ref} - \frac{V_C V_G}{x_{eq}} \sin\delta) \tag{6}$$

$$x_{eq} = x_f + x_{tr} + x_1 \| x_2 \tag{7}$$

where V_C and V_G are the rms values of converter and infinite bus line-to-line voltages, respectively. Weakness of the grid can be defined by the short circuit ratio (SCR) as:

$$SCR = \frac{1}{x_{eq}[p.u.]} \tag{8}$$

The weakness of the grid represented by the SCR value imposes limitations on the margins of stability in the system. The high-impedance of the grid during grid faults jeopardize the transient stability of the grid-connected converter system. In the situation of a fault in a weak grid, two main points should be taken into account. First, the high impedance of the grid brings down the deliverable active power. Second, the voltage dip in the grid demands voltage support by the converter. Whereas, the synchronization mechanism of PSC is based on the active power, so the reactive power controller for grid voltage support is an outer loop of the control system with a slow dynamic response.

In brief, the transient stability of the grid-connected system is contingent on the dynamic response of the power angle δ. Following the grid fault, two different dynamic responses are probable. First, a new stable operating point is obtained. Second, the power angle of the converter diverges and causes instability in the system. Severity and duration of the grid fault, weakness of the grid, and the pre-fault operating point of the converter are the main factors that determine the transient stability of the system. PSC lacks virtual inertia which results in a first-order differential equation modelling the dynamics of the synchronization loop. In addition, the time-constant of the synchronization loop is smaller than that of a synchronous machine. These properties imply that the fault-clearance time plays an integral role in the transient stability of PSC. By solving (6), the trajectory of the power angle and an estimation of the critical fault-clearance time t_{crt} can be obtained as:

$$t_{crt} = \int dt = \int_{\delta_0}^{\pi/2} \frac{d\delta}{K_{ip}\left(P_{ref} - \frac{V_C V_G}{x_{eq}}\right)\sin\delta} \tag{9}$$

Considering the parameters listed in Table I, in case of a 0.6 p.u. voltage dip due to a grid fault, the grid-connected converter system loses synchronization and becomes unstable even with a short fault-clearance time. The phase-portrait of the system for the pre-fault and during-fault operation is depicted in Fig. 1 (c) for such a situation.

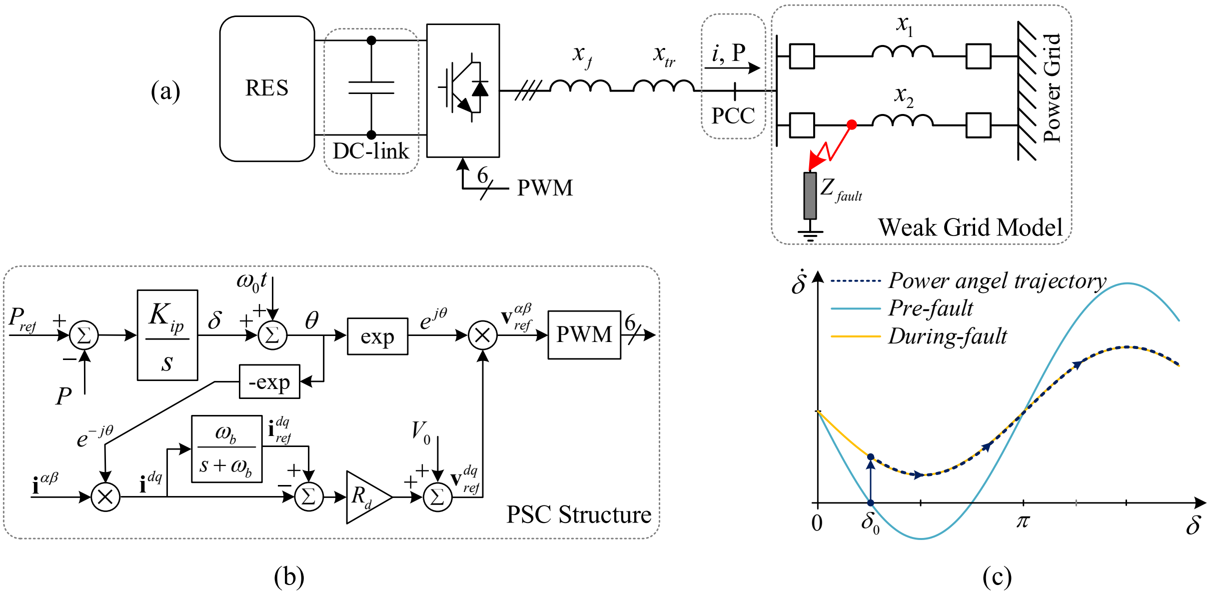

Fig. 1: Three-phase grid-connected converter system controlled by PSC (a) Three-phase voltage-source converter connected to a high-impedance grid, (b) the control structure of PSC, and (c) trajectory of the converter power angle during grid faults.

PCC voltage trajectory during grid faults

In a grid-connected converter system with low SCR, following a voltage drop in the grid, the voltage at the PCC will drop as well. During the very first moments, the control system attempts to keep up the voltage of the PCC by increasing the internal voltage of the converter. However, in the case of a severe voltage drop, the converter loses synchronization with the grid. The trajectory of PCC voltage is demonstrated in Fig. 2 for two different faults in the grid.

The case that the converter remains stable during fault is demonstrated in Fig. 2 (a) for a couple of pre-fault operating conditions. In this case, the converter delivers reactive power to support the grid voltage without loss of synchronization and helps voltage recovery of the grid. On the other hand, for a more severe voltage drop, although the converter attempts to increase the internal voltage and support the grid voltage, due to the loss of synchronization, the converter becomes unstable and the PCC voltage starts fluctuating as depicted in Fig. 2 (b).

Table I: Specifications of the grid-connected converter system

Parameter	Description	Value
x_f	Reactance of the converter filter	0.07 [p.u]
x_1	Reactance of line 1	0.8 [p.u.]
x_2	Reactance of line 2	0.8 [p.u.]
x_{tr}	Reactance of the transformer	0.057 [p.u.]
K_{ip}	PSL integrator gain	0.01 [p.u.]
R_d	Active-damping gain	0.2 [p.u.]
ω_d	Active-damping bandwidth	100 [rad/s]
ω_0	Power system angular frequency	100π [rad/s]

As shown in Fig. 2, stable operation of the converter during grid faults is contingent on the severity of the voltage drop and the pre-fault operating point of the converter which is a function of the grid impedance as well. By extracting the pattern of the PCC voltage trajectory, it would be possible to analyze and predict the transient stability of the grid-connected converter system following a grid fault.

The trajectory of the PCC voltage after the fault occurrence reveals that whether the converter is able to support the grid voltage without loss of synchronization or not.
Following the voltage drop, if the voltage recovery begins, it shows that the converter will be successful in supporting the grid voltage and continue stable operation. On the other hand, after the voltage drop if the voltage recovery fails, it shows that the converter will collapse and lose synchronization.
Consequently, in this paper by means of deep learning methods, the trajectory of the PCC voltage is extracted, analyzed, and predicted in order to modify the active power reference, the internal voltage, and the synchronization loop of the converter to enhance the transient stability of PSC-controlled converters. The employed deep learning method is presented in the next section.

Analyzing and forecasting the PCC voltage trajectory by LSTM

To address the PCC voltage trajectory extraction and analysis, this paper employs LSTM architecture which provides a straightforward processing of order among samples of a sequence. LSTM processes the order of the sampled data when learning a mapping from observations (input data) to the output [11], [12]. This capability of learning the order of the data is not offered by multilayer perceptron (MLP) or convolutional neural networks (CNN).

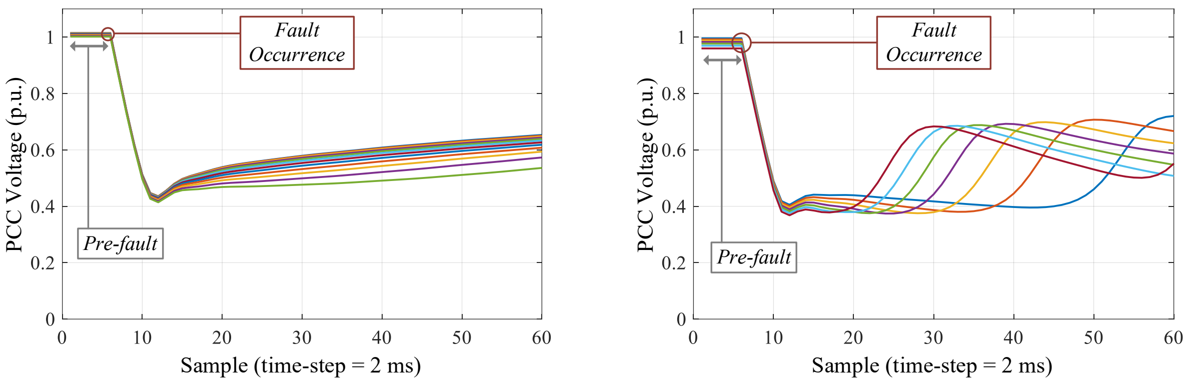

(a) (b)

Fig. 2: PCC voltage trajectory during faults in a weak grid (a) stable operation of the converter during voltage drop, and (b) transient instability in the converter and loss of synchronization with the grid.

Among neural networks, LSTM architecture introduces inherent advantages for handling sequences and time-series. LSTM learns to map the inputs over time to an output and captures the dependences of observations with large time step distances. Furthermore, LSTM is suitable for time-series prediction using time-window techniques and naturally learns the temporal dependence from the input observations. Because of these merits over other neural network architectures, it is reasonable to employ LSTM, which can learn long-term correlations among PCC voltage samples as a sequence of observations, in this application. Thus, the most prominent context of the PCC voltage samples to the expected output (i.e. PCC voltage trajectory) would be extracted and learned and can be modified dynamically to continue the given sequence. In the following, the proposed LSTM network with deep architecture and multiple hidden layers is described. Structure of an LSTM cell is depicted in Fig. 3.

LSTM neural networks

The input data of the employed LSTM network are samples of the PCC voltage at the current time step $\mathbf{V}_t$ and the hidden state of the preceding time step $\mathbf{H}_{t-1}$, as shown in Fig. 3. The concatenated data of $\mathbf{V}_t$ and $\mathbf{H}_{t-1}$ are processed by three fully connected (FC) layers including input gate, forget gate, and output gate. Each FC layer has an activation function with the type of sigmoid σ or hyperbolic tangent $\tanh$ to compute the values of the subsequent gates. The sigmoid activation function maps the values of the input gate, forget gate, and output gate to the range of $(0,1)$.
The number of hidden units is h and the batch size is k. By assuming that the number of inputs is l, the input at the current time step would be $\mathbf{V}_t \in \mathbb{R}^{k \times l}$. Thus, the hidden state of the preceding time step is $\mathbf{H}_{t-1} \in \mathbb{R}^{k \times h}$. Similarly, the gates at the current time step t can be defined as the input gate $\mathbf{I}_t \in \mathbb{R}^{k \times h}$, the forget gate $\mathbf{F}_t \in \mathbb{R}^{k \times h}$, and the output gate $\mathbf{O}_t \in \mathbb{R}^{k \times h}$ given by:

$$\mathbf{I}_t = \sigma\left(\mathbf{V}_t\mathbf{W}_{vi} + \mathbf{H}_{t-1}\mathbf{W}_{hi} + \mathbf{b}_i\right)$$
$$\mathbf{F}_t = \sigma\left(\mathbf{V}_t\mathbf{W}_{vf} + \mathbf{H}_{t-1}\mathbf{W}_{hf} + \mathbf{b}_f\right) \tag{10}$$
$$\mathbf{O}_t = \sigma\left(\mathbf{V}_t\mathbf{W}_{vo} + \mathbf{H}_{t-1}\mathbf{W}_{ho} + \mathbf{b}_o\right)$$

where $\mathbf{W}_{vi}, \mathbf{W}_{vf}, \mathbf{W}_{vo} \in \mathbb{R}^{l\times h}$ and $\mathbf{W}_{hi}, \mathbf{W}_{hf}, \mathbf{W}_{ho} \in \mathbb{R}^{h\times h}$ are the weight parameters for the input, forget, and output gates, respectively. The bias parameters are denoted by $\mathbf{b}_i, \mathbf{b}_f, \mathbf{b}_o \in \mathbb{R}^{1\times h}$ for the input, forget, and output gates, respectively. Prospect memory cell $\mathbf{P}_t$ is another element of LSTM computed by tanh resulting a value in the range of $(-1,1)$ at the time step t as:

$$\mathbf{P}_t = \tanh\left(\mathbf{V}_t\mathbf{W}_{vp} + \mathbf{H}_{t-1}\mathbf{W}_{hp} + \mathbf{b}_p\right) \tag{10}$$

where $\mathbf{W}_{vp} \in \mathbb{R}^{l\times h}$ and $\mathbf{W}_{hp} \in \mathbb{R}^{h\times h}$ are weight parameters and $\mathbf{b}_c \in \mathbb{R}^{1\times h}$ is a bias parameter for computing the prospect memory cell $\mathbf{P}_t$ at the current time step. In LSTM there are two dedicated gates for governing input and forgetting purposes. The input gate $\mathbf{I}_t$ determines how much of the new data should be taken into account by means of $\mathbf{P}_t$. The forget gate $\mathbf{F}_t$ addresses what portion of the preceding memory cell content $\mathbf{M}_{t-1} \in \mathbb{R}^{k\times h}$ should be retrain. Correspondingly, the memory cell $\mathbf{M}_t$ can be defined by:

$$\mathbf{M}_t = \mathbf{F}_t \odot \mathbf{M}_{t-1} + \mathbf{I}_t \odot \mathbf{P}_t. \tag{11}$$

The hidden state $\mathbf{H}_t \in \mathbb{R}^{k\times h}$ in LSTM is considered as a gated type of the memory cell content $\mathbf{M}_t$ with an activation function tanh as:

$$\mathbf{H}_t = \mathbf{O}_t \odot \tanh(\mathbf{M}_t) \tag{12}$$

thereby, the values of $\mathbf{H}_t$ are all in the range of $(-1,1)$. Finally, the flow diagram of the LSTM network used in this work is depicted in Fig. 3.

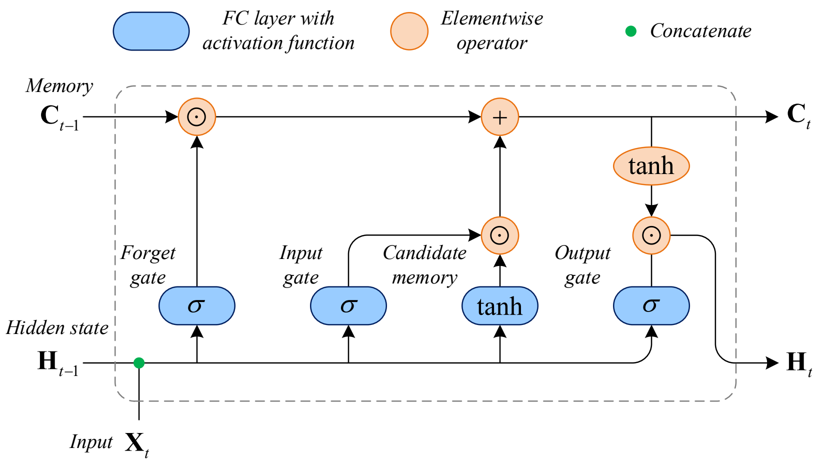

Fig. 3: Architecture of a cell in an LSTM network.

Training, evaluation, and application

A large number of contingencies simulated in MATLAB/Simulink has been used for training the LSTM network. The training data consists of various pre-fault operating condition, a wide range of grid SCR values, and a large collection of short-circuit fault impedances summarised in Table 2. Three-phase to ground faults at various locations were simulated and the trajectory of PCC voltage and stability condition of the converter were logged. It was assumed that the short-circuit faults could be cleared after five cycles by disconnecting the faulted line, as shown in Fig. 1 (a). This resulted in 25000 simulation cases where 37% of the logged data are related to the case that the loss of synchronization happens. From the recorded data, 75% of stable cases and 75% of unstable cases were randomly dedicated to training the network. The remaining 25% of the recorded data were used for evaluation of the trained network.

The PCC voltage samples were collected at a sampling period $T_s = 2ms$ during a time interval including pre-fault and during-fault operation of the converter. Consequently, a proper dataset was generated to train the LSTM network for achieving an accurate voltage trajectory extraction and prediction.

To evaluate the prediction accuracy of the trained LSTM, the root mean squared normalized error (RMSE) is considered as the performance index. Sampled PCC voltages and the output of the trained LSTM for two different cases are shown in Fig. 4. First, the case that the converter continues operation without loss of synchronization after the fault occurrence as shown in Fig. 4 (a). Second, the case that the converter loses synchronization and becomes unstable after the grid-fault.
Accuracy of the trained LSTM network is illustrated in Fig. 4 (c) and (d) by calculating the RMSE value of each voltage trajectory forecast. The calculated RMSE reveals that the trained LSTM can extract and predict the PCC voltage trajectory regardless of uncertainty existing in data and missing values of data points. The proposed LSTM network is trained offline by the generated data coming from time-domain simulations for various grid conditions and grid faults. Since the LSTM network has been trained, it can be used in the synchronization loop of PSC to adapt the active power error with the grid operating condition, which is presented in the next section.

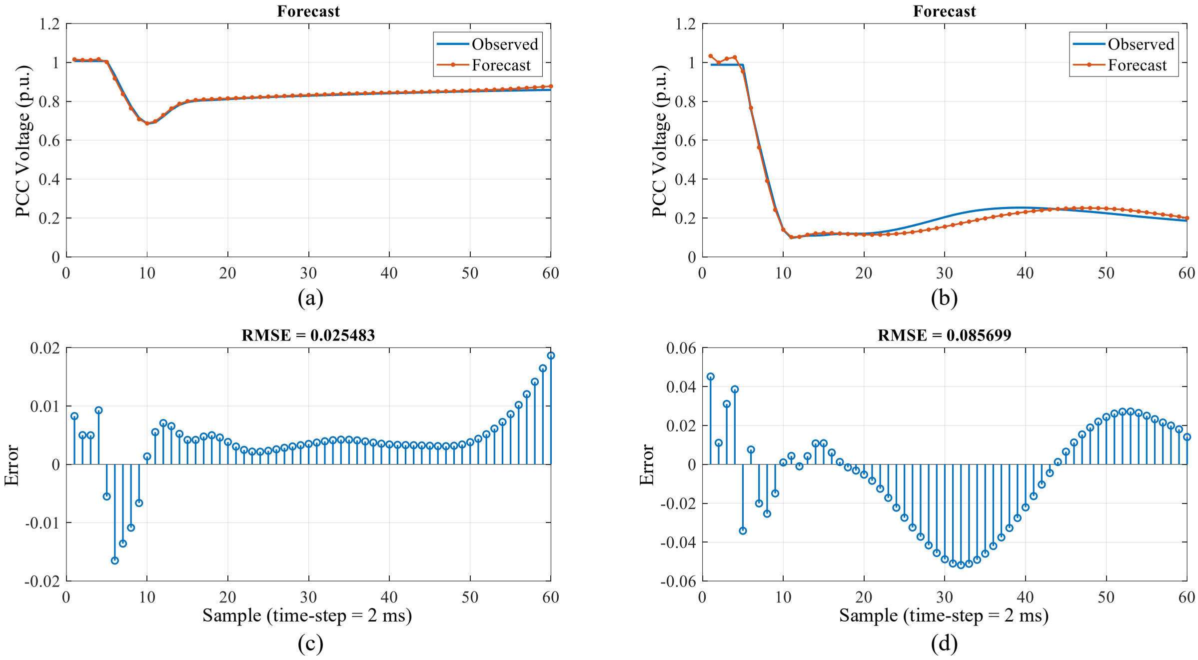

Fig. 4: Comparison of the sampled PCC voltage and the LSTM forecast (a) PCC voltage trajectory during stable operation of the converter, (b) PCC voltage trajectory during loss of synchronization in the system, (c) forecast error of the LSTM network for the former case, and (d) forecast error for the latter case.

Table II: Specifications of the trained LSTM network

Parameter	Description	Value
l	Number of inputs (look back samples)	10
h	Number of hidden layers	75
k	Batch size	25
Epochs	Number of epochs	500
RMSE	Normalized RMSE of network training	0.021468

Online adaptation of PSC with grid condition

The objective of this section is to enhance the transient stability of PSC by updating the references of the control system based on the extracted PCC voltage trajectory via LSTM. During grid faults, both

LVRT requirements and stable operation of the converters should be achieved. By extracting and predicting the PCC voltage trajectory, presented in the previous section, new references for the delivered active power and the internal voltage of the converter can be calculated.

The LSTM network processes the PCC voltage samples and generates the PCC voltage trajectory v_{LSTM}. The amplitude of the converter current I_C can be expressed by:

$$I_C = \frac{V_0 - V_{pcc}\angle\alpha}{x_f} \tag{13}$$

where, V_{pcc} and α are the amplitude and angle of the PCC voltage respectively. The impedance of the converter output filter x_f is small enough to assume that the phase difference between the internal voltage of the converter and the voltage of PCC is negligible $(\alpha \approx 0)$. Thus, the internal voltage of the converter during grid faults for delivering the rated current to the grid can be expressed by:

$$V_{ad} \approx x_f I_C^{rated} + v_{LSMT} \tag{14}$$

where, V_{ad} is the required internal voltage of the converter during grid faults, I_C^{rated} is the rated current of the converter, and v_{LSTM} is the processed value of the PCC voltage amplitude by the trained LSTM network. Next, by considering the LVRT requirements (discussed in [14] for power-angle synchronization control) and the capacity of the converter, new reference signals for PSC can be calculated dynamically as:

$$V_{ad} = \begin{cases} V_0 & v_{LSMT} > 0.9 \\ x_f I_C^{rated} + v_{LSMT} & v_{LSTM} < 0.9 \end{cases} \tag{15}$$

$$P_{ad} = \begin{cases} V_0 & v_{LSMT} > 0.9 \\ \min\{P_{ref}, P_{LVRT}\} & v_{LSTM} < 0.9 \end{cases} \tag{16}$$

where, P_{ad} and P_{ref} are the grid-fault-adapted and pre-fault active power reference for PSC, respectively; P_{LVRT} is the maximum allowed active power reference in accordance with the LVRT requirements. The modified control system is demonstrated in Fig. 5.

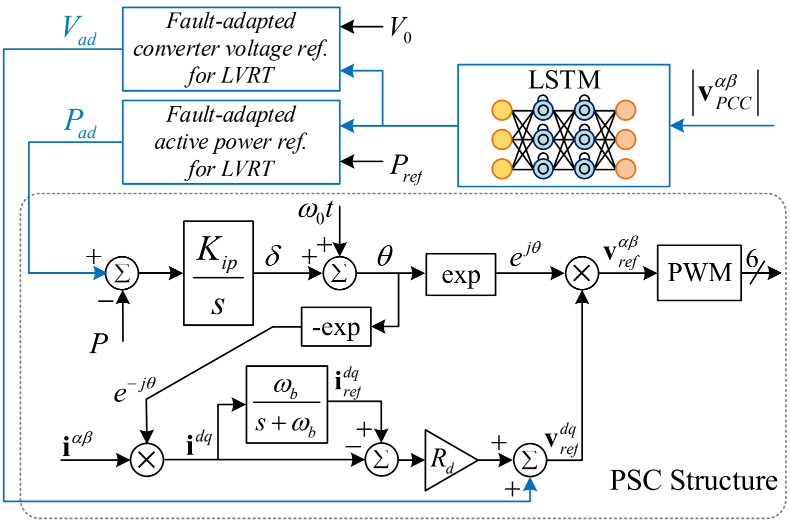

Fig. 5: LSTM-integrated PSC

Simulation and evaluation

Time-domain simulations carried out in MATLAB/Simulink are presented in this section to demonstrate the effectiveness of the proposed solution for enhancing the transient stability of PSC. The simulated grid-connected converter system is the same as the one shown in Fig. 1 (a). In order to evaluate the proposed modified control system, both of the conventional PSC (as shown in Fig. 1 (b)) and the modified PSC (as shown in Fig. 5) were simulated. A short circuit fault happens, and the grid voltage drops to less than 50% of the rated value. In this situation, the converter should deliver reactive power to support the grid voltage in accordance to the LVRT requirements. Two case studies are presented in the following.

Case study I: conventional PSC

Simulation results of the grid-connected converter system with PSC is presented in Fig. 6 (a), (b), and (c). The PCC voltage drops following the grid fault and starts fluctuating due to the loss of synchronization between the converter and the grid. This imposes excessive current flow to the grid by the converter which leads to converter collapse.

Case study II: LSTM-integrated PSC

In this case, the trained LSTM network is used to update the active power reference and the internal voltage setpoint of the control system during the grid fault. Simulation results presented in Fig. 6 (d), (e), and (f) shows that the modified control system can handle the fault situation as well as maintaining synchronization with the grid. Consequently, the LVRT requirements are satisfied and the stable operation of the grid-connected converter system is achieved.
In summary, by employing LSTM for processing the trajectory of the PCC voltage, references of the control system would be updated dynamically, preventing the loss of synchronization in the grid-connected converter system. Fig. 6 shows a close match between the proposed theoretical analysis and the obtained simulation results.

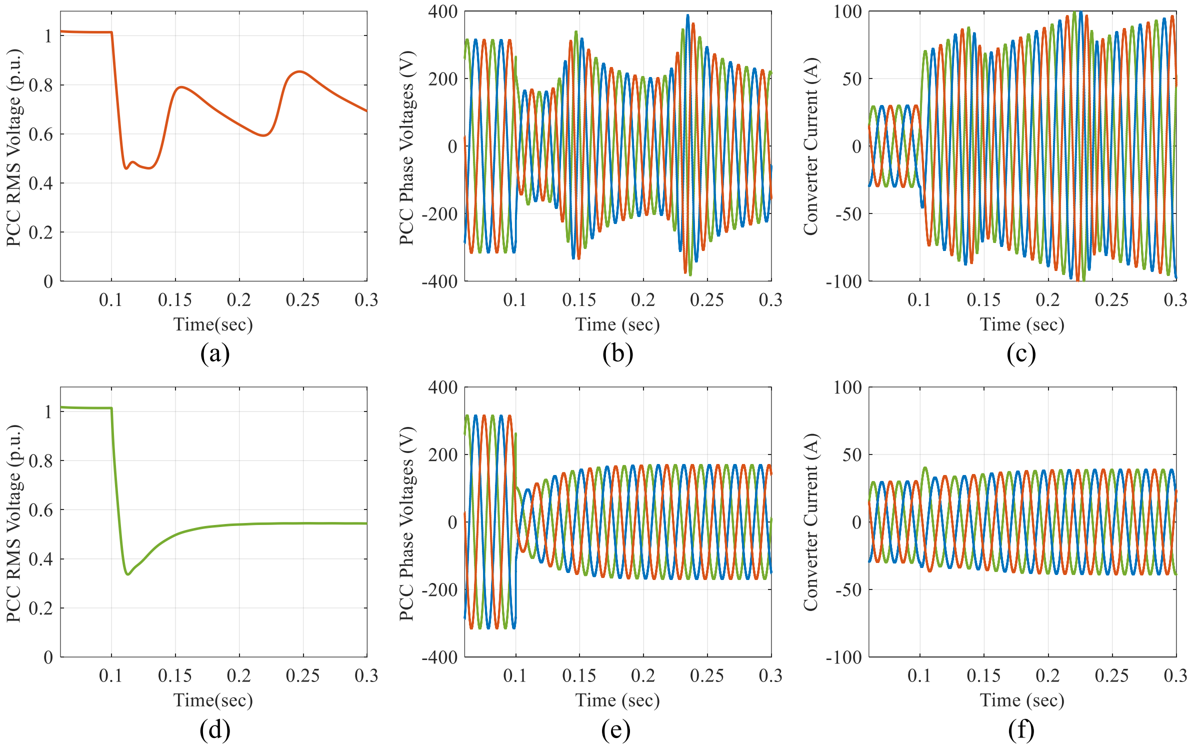

Fig. 6: Time-domain simulation results of the grid-connected converter system during grid faults (a) PCC voltage trajectory of case study I, (b) phase voltages of case study I, (c) converter currents of case study I, (d) PCC voltage trajectory of case study II, (e) phase voltages of case study II, and (f) converter currents of case study II.

Conclusion

This paper proposed a deep learning-based method to enhance the transient stability of PSC during grid faults and satisfy the LVRT requirements as well. To achieve this, the control system has been developed by integrating a trained LSTM network for extraction and prediction of the PCC voltage to update dynamically the active power reference and the internal voltage of the converter for prevention of loss of synchronization. The superior performance of the developed control system has been demonstrated by time-domain simulations of a grid-connected converter system with contingencies. By the proposed LSTM-integrated PSC, the control system maintains the synchronization with the grid during faults, and the stable operating of the converter can be achieved.

References

[1] Pouresmaeil M., Sepehr A., Sangrody R., Taheri S., Pouresmaeil E.: Control of multilevel converters for high penetration of renewable energies, PEDG 2021, paper 84

[2] Zhang L., Harnefors L., and Nee H. P.: Power-synchronization control of grid-connected voltage-source converters, IEEE Transactions on Power Systems Vol 25 no 2, pp. 809- 820

[3] Huang L. et al.: Grid-synchronization stability analysis and loop shaping for PLL-based power converters with different reactive power control, IEEE Transactions on Smart Grid Vol 11 no 1, pp. 501- 516

[4] Hagmar H., Tong L., Eriksson R., and Tuan L. A.: Voltage instability prediction using a deep recurrent neural network, IEEE Transactions on Power Systems Vol 36 no 1, pp. 17- 27

[5] Sepehr A., Pouresmaeil E., Saeedian M., Routimo M., Godina R., and Yousefi-Talouki A.: Control of grid-tied converters for integration of renewable energy sources into the weak grids, SEST 2019, paper 213

[6] Taul M. G., Wang X., Davari P., and Blaabjerg F.: An overview of assessment methods for synchronization stability of grid-connected converters under severe symmetrical grid faults, IEEE Transactions on Power Electronics Vol 34 no 10, pp. 9655- 9670

[7] Cheng H., Shuai Z., Shen C., Liu X., Li Z., and John Shen Z.: Transient angle stability of paralleled synchronous and virtual synchronous generators in islanded microgrids, IEEE Transactions on Power Electronics Vol 35 no 8, pp. 8751- 8765

[8] Sepehr A., Pouresmaeil M., Hojabri M., Blaabjerg F., and Pouresmaeil E.: Improving transient stability of power synchronization control for weak grid applications, COMPEL 2020, paper 269

[9] Wu H. and Wang X.: Design-oriented transient stability analysis of grid-connected converters with power synchronization control, IEEE Transactions on Industrial Electronics Vol 66 no 8, pp. 6473- 6482

[10] Shuai Z. et al.: Transient angle stability of virtual synchronous generators using Lyapunov's direct method, IEEE Transactions on Smart Grid Vol 10 no 4, pp. 4648- 4661

[11] Farsi B., Amayri M., Bouguila N., and Eicker U.: On short-term load forecasting using machine learning techniques and a novel parallel deep LSTM-CNN approach, IEEE Access Vol 9, pp. 31191- 31212

[12] Alazab M., Khan S., Krishnan S. S. R., Pham Q., Reddy M. P. K., and Gadekallu T. R.: A multidirectional LSTM model for predicting the stability of a smart grid, IEEE Access Vol 8, pp. 85454- 85463

[13] Harnefors L., Hinkkanen M., Riaz U., Rahman F. M. M., and Zhang L.: Robust analytic design of power-synchronization control, IEEE Transactions on Industrial Electronics Vol 66 no 8, pp. 5810- 5819

[14] Lee C., Hsu C., and Cheng P.: A low-voltage ride-through technique for grid-connected converters of distributed energy resources, IEEE Transactions on Industry Applications Vol 47 no 4, pp. 1821- 1832